Hale COLLAGE 2017 Lecture 15

Flare loop observations: imaging and spectroscopy II

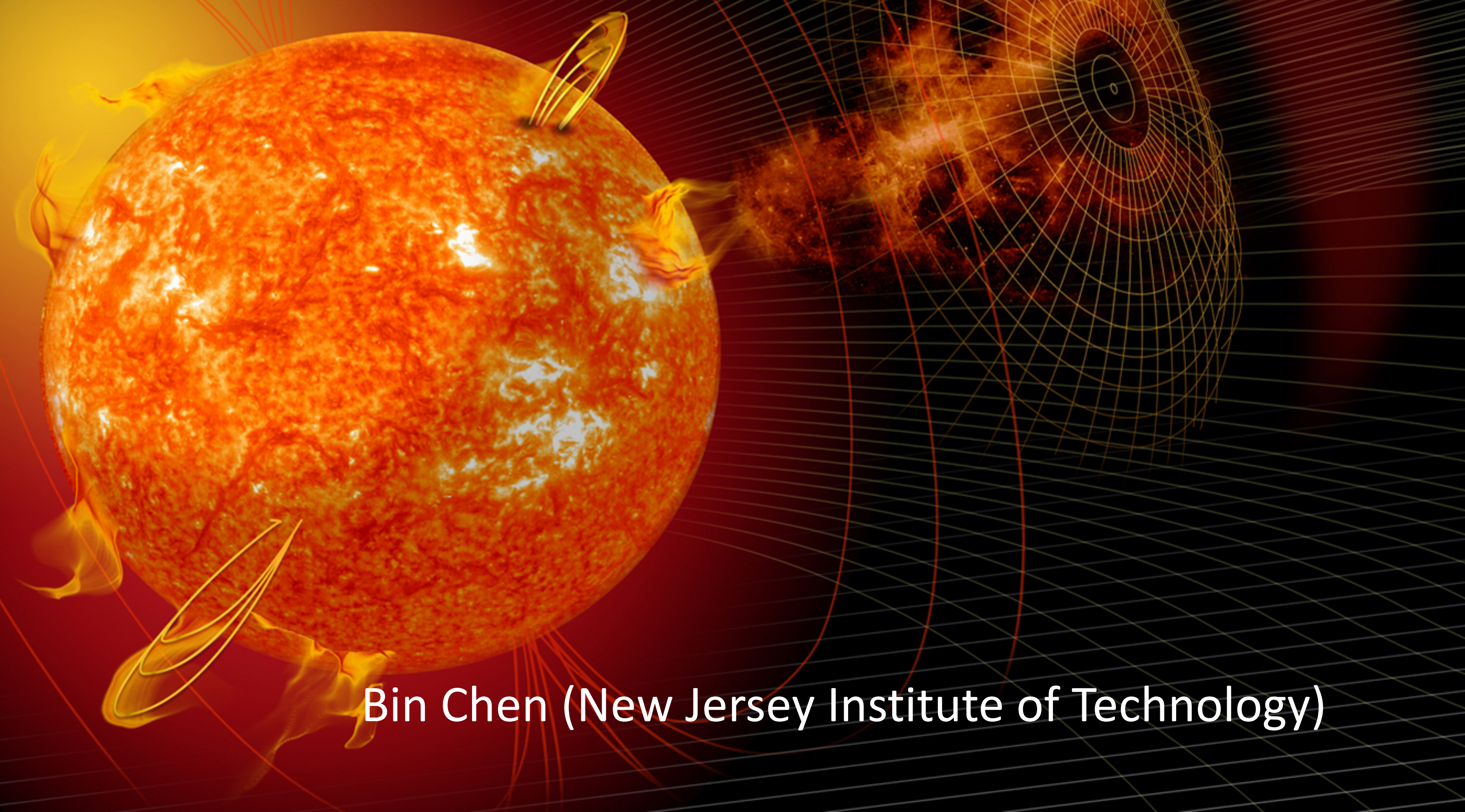

Bin Chen (New Jersey Institute of Technology)

Outline

- Flare spectroscopy*
  - Review on some fundamentals
    - Atomic structure
    - line diagnostics
    - Suggested reading: Ch. 3 of P. Foukal, Ch. 2 of Tandberg-Hanssen & Emslie
  - Examples of flare spectroscopic observations
    - Chromospheric evaporation
    - Reconnection site

* This lecture focuses on optically thin (E)UV lines

Atomic energy levels

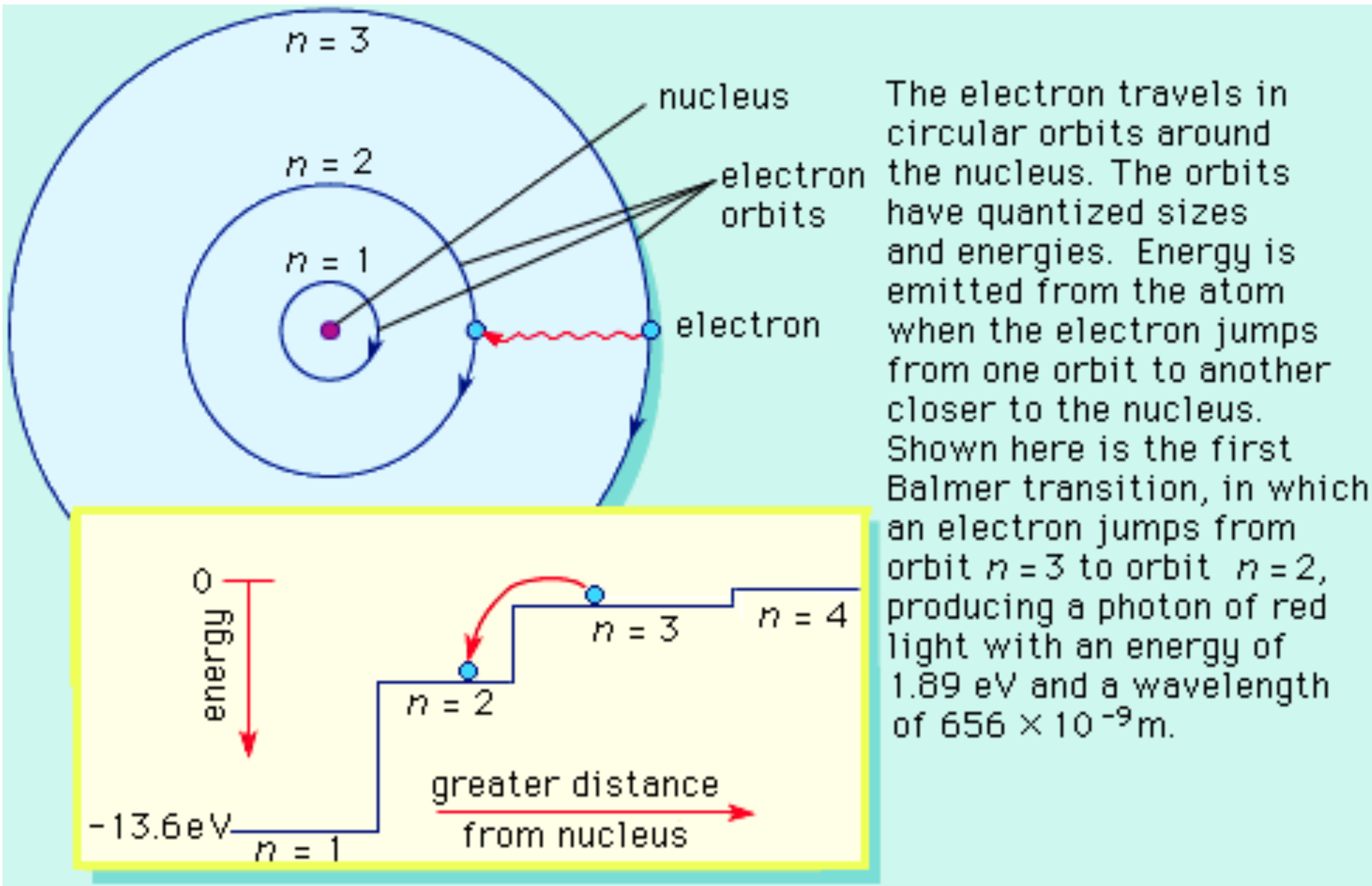

An hydrogen atom

Atomic levels of hydrogen: principle quantum number n

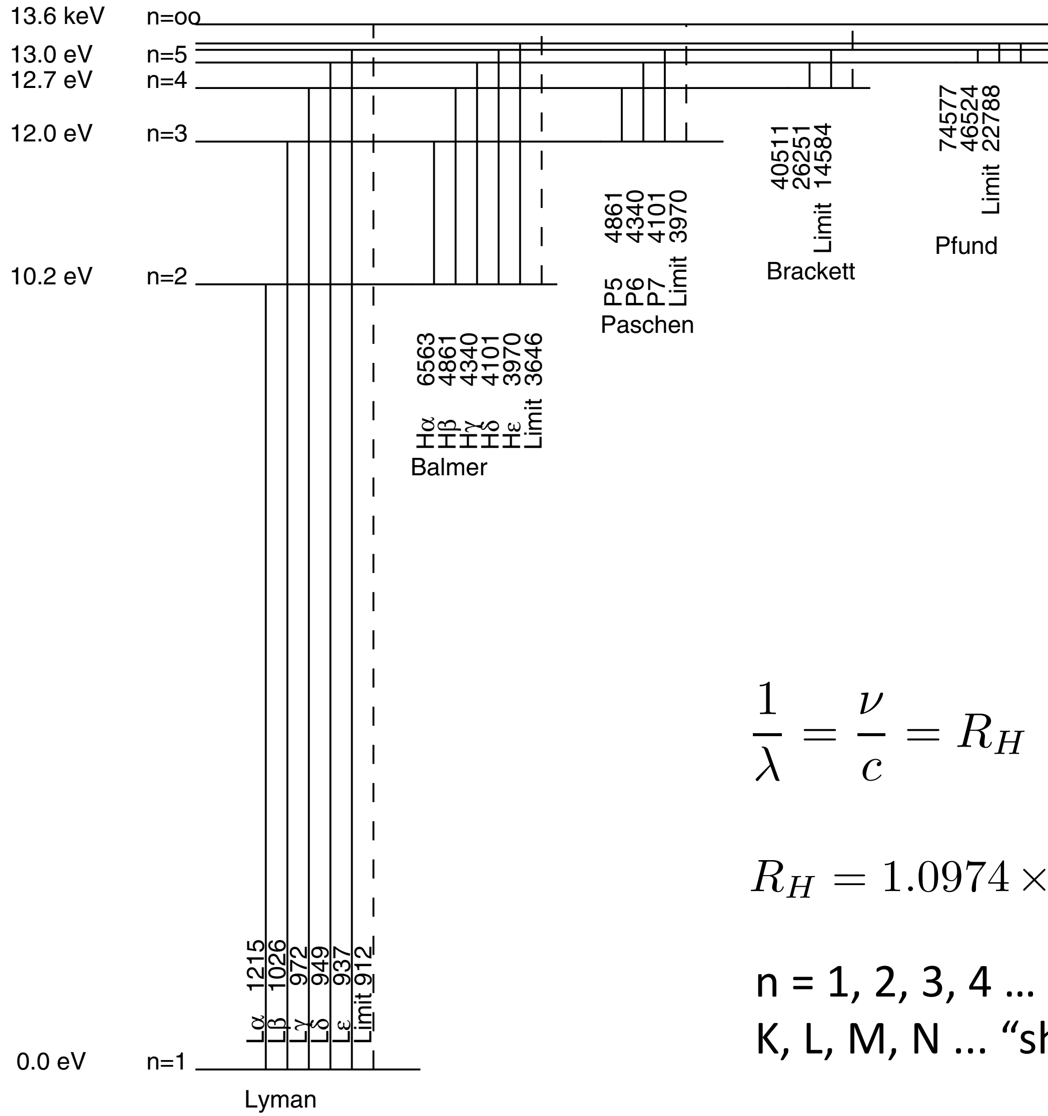

$$\frac{1}{\lambda} = \frac{\nu}{c} = R_H \left[\frac{1}{n_1^2} - \frac{1}{n_2^2} \right]$$

$$R_H = 1.0974 \times 10^5 \text{ cm}^{-1}$$

n = 1, 2, 3, 4 … are also labeled as K, L, M, N ... “shells”

Atomic levels of hydrogen: orbital angular quantum number l

- As the energy levels increase, so do the number of "subshells" which are associated with the *orbital angular momentum*.
- $l = 0, 1, \dots, n-1$, labelled as *s, p, d, f, g, h, i …*
  - The **first** energy level (n=1) has **1** subshell (s)
  - The **second** energy level (n=2) has **2** subshells (s & p)
  - The **third** energy level (n=3) has **3** subshells (s, p, & d)

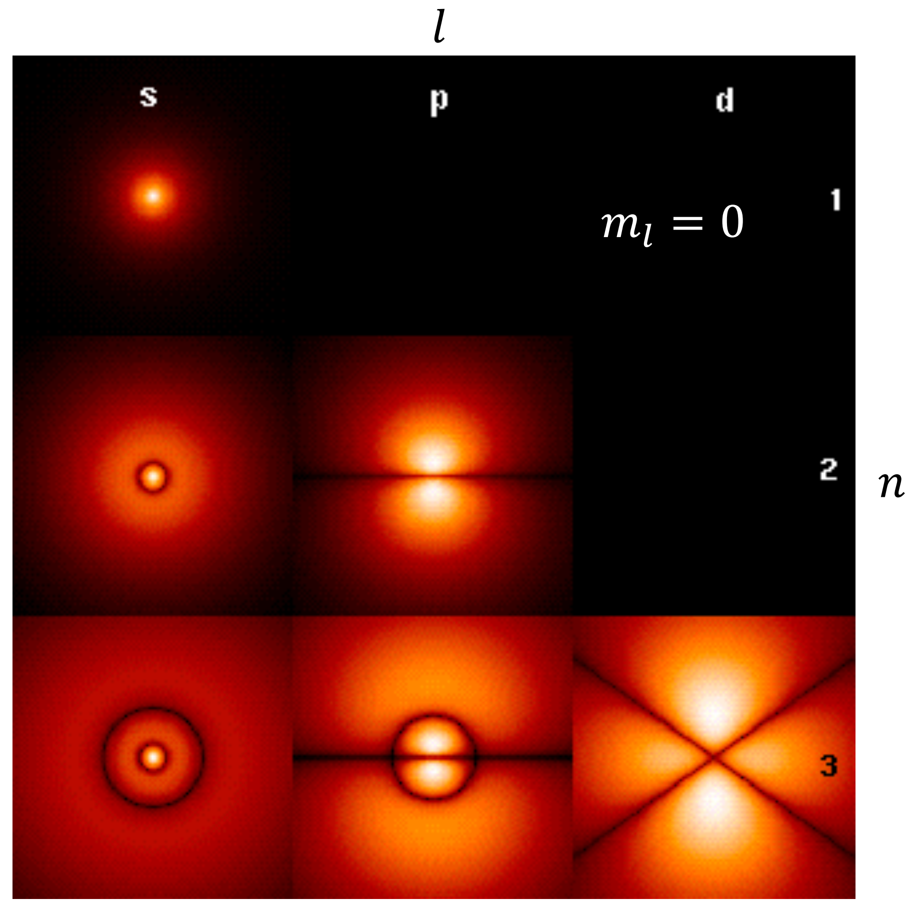

Probability densities for a hydrogen electron

Atomic levels of hydrogen: Additional quantum numbers m_l, m_s

- m_l: magnetic (or projected) quantum number of the angular momentum, from $-l$ to l, including 0

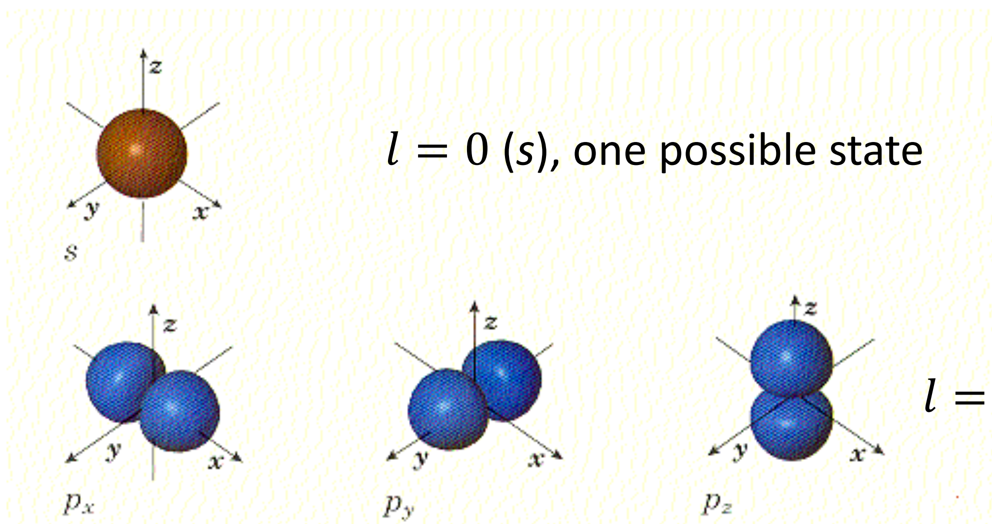

$l = 0$ (s), one possible state

$l = 1$ (p), three possible states

- m_s: spin quantum number, −½ or ½ for a single electron

Spin up

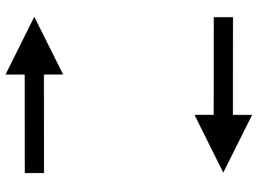

Spin down

Two possible states

Spectroscopic notation

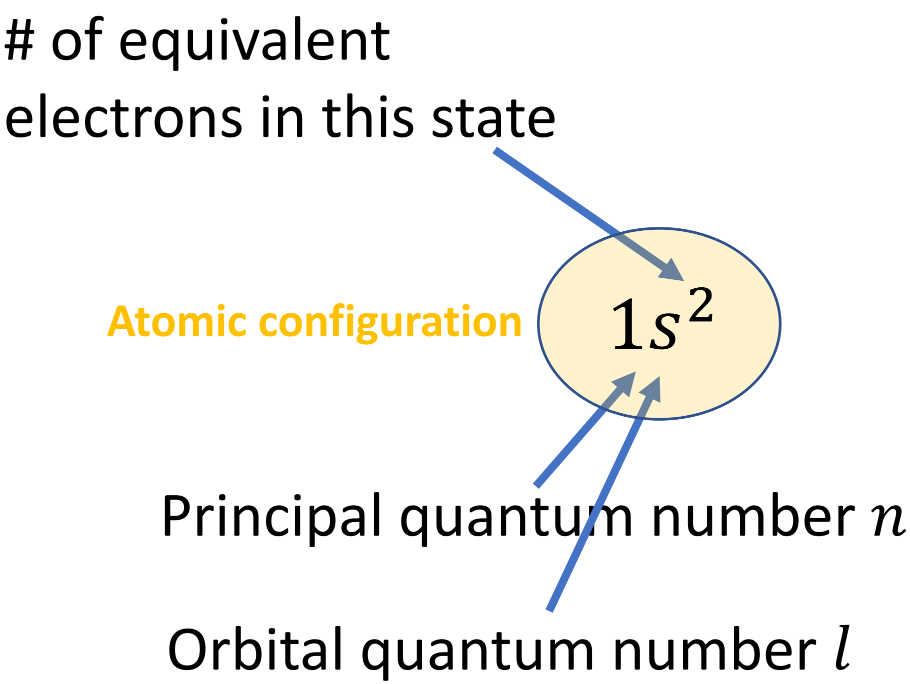

Element	Symbol	Z	Ground configuration
Hydrogen	H	1	$1s$
Helium	He	2	$1s^2$
Lithium	Li	3	$1s^2 2s$
Beryllium	Be	4	$1s^2 2s^2$
Boron	B	5	$1s^2 2s^2 2p$
Carbon	C	6	$1s^2 2s^2 2p^2$
Nitrogen	N	7	$1s^2 2s^2 2p^3$
Oxygen	O	8	$1s^2 2s^2 2p^4$
Fluorine	F	9	$1s^2 2s^2 2p^5$
Neon	Ne	10	$1s^2 2s^2 2p^6$
Sodium	Na	11	$1s^2 2s^2 2p^6 3s$
Potassium	K	19	$1s^2 2s^2 2p^6 3s^2 3p^6 4s$
Calcium	Ca	20	$1s^2 2s^2 2p^6 3s^2 3p^6 4s^2$
Vanadium	V	23	$1s^2 2s^2 2p^6 3s^2 3p^6 4s^2 3d^3$
Chromium	Cr	24	$1s^2 2s^2 2p^6 3s^2 3p^6 4s 3d^5$
Iron	Fe	26	$1s^2 2s^2 2p^6 3s^2 3p^6 4s^2 4p^6$

Table 2.1 of Aschwanden's book

Spin-orbit interaction and fine structure splitting

- Hydrogen Lyman-α line

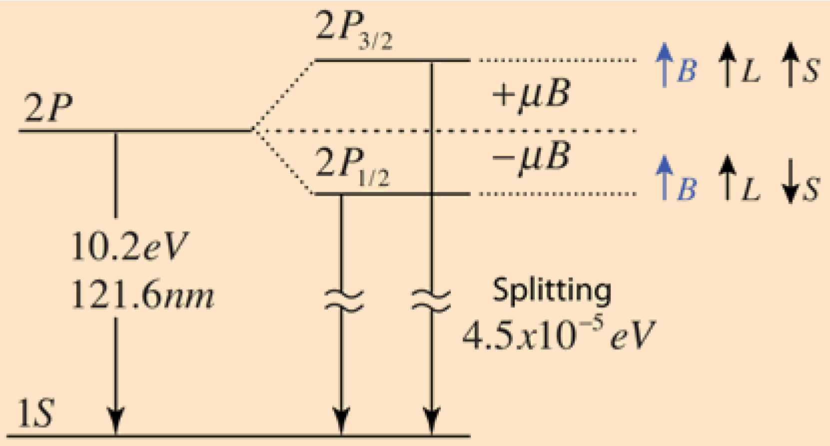

The small splitting of the spectral line is attributed to an interaction between the electron spin S and the orbital angular momentum L. It is called the spin-orbit interaction.

- Multi-electron system:
  - Total orbital angular momentum: $\boldsymbol{L} = \sum \boldsymbol{l}_i$
  - Total spin angular momentum: $\boldsymbol{S} = \sum \boldsymbol{s}_i$
  - Total angular momentum: $\boldsymbol{J} = \boldsymbol{L} + \boldsymbol{S}$
  - Total angular momentum number J ranges from $|L - S|$ to $L + S$
  - Multiplicity or “terms”: $r = 2S + 1$

Spectroscopic notation: term symbol

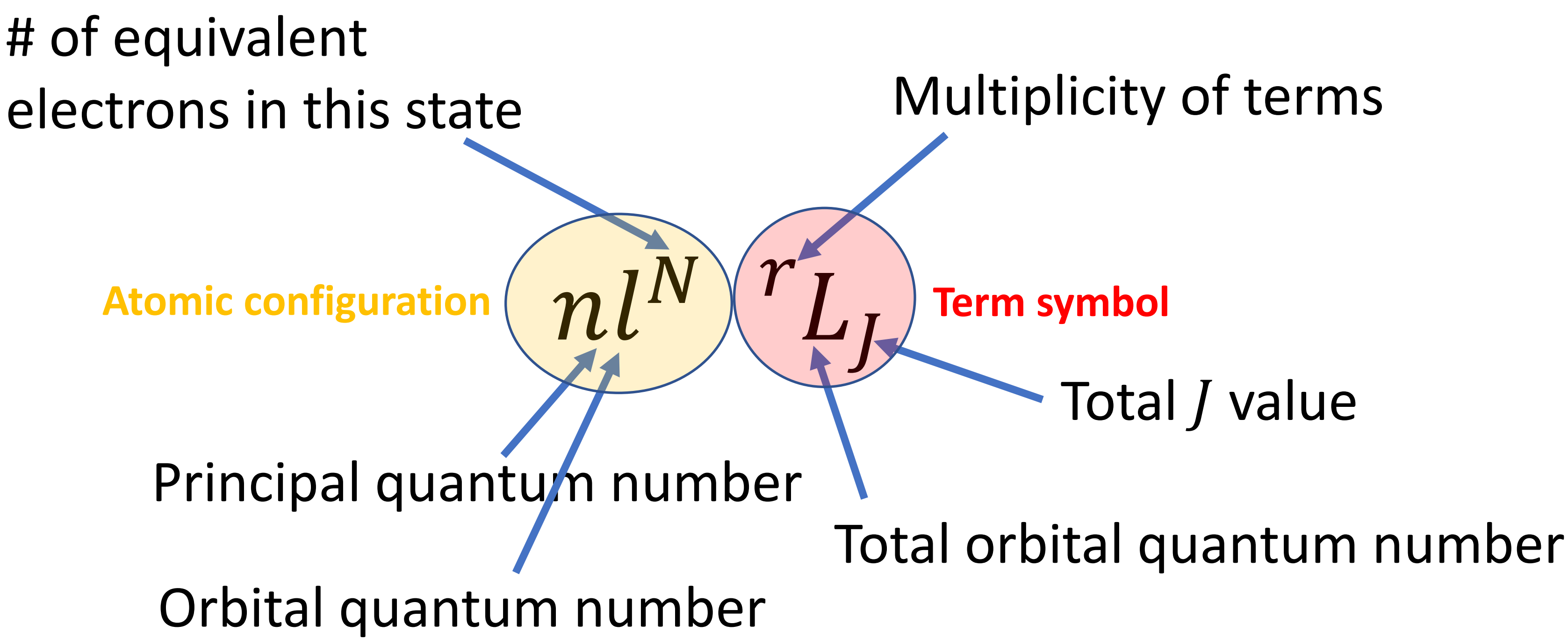

Example: ground state of Na I is $1s^2 2s^2 2p^6 3s \;\; {}^2S_{1/2}$

Line transition and selection rules

Grotrian diagram (or term diagram) for atomic hydrogen

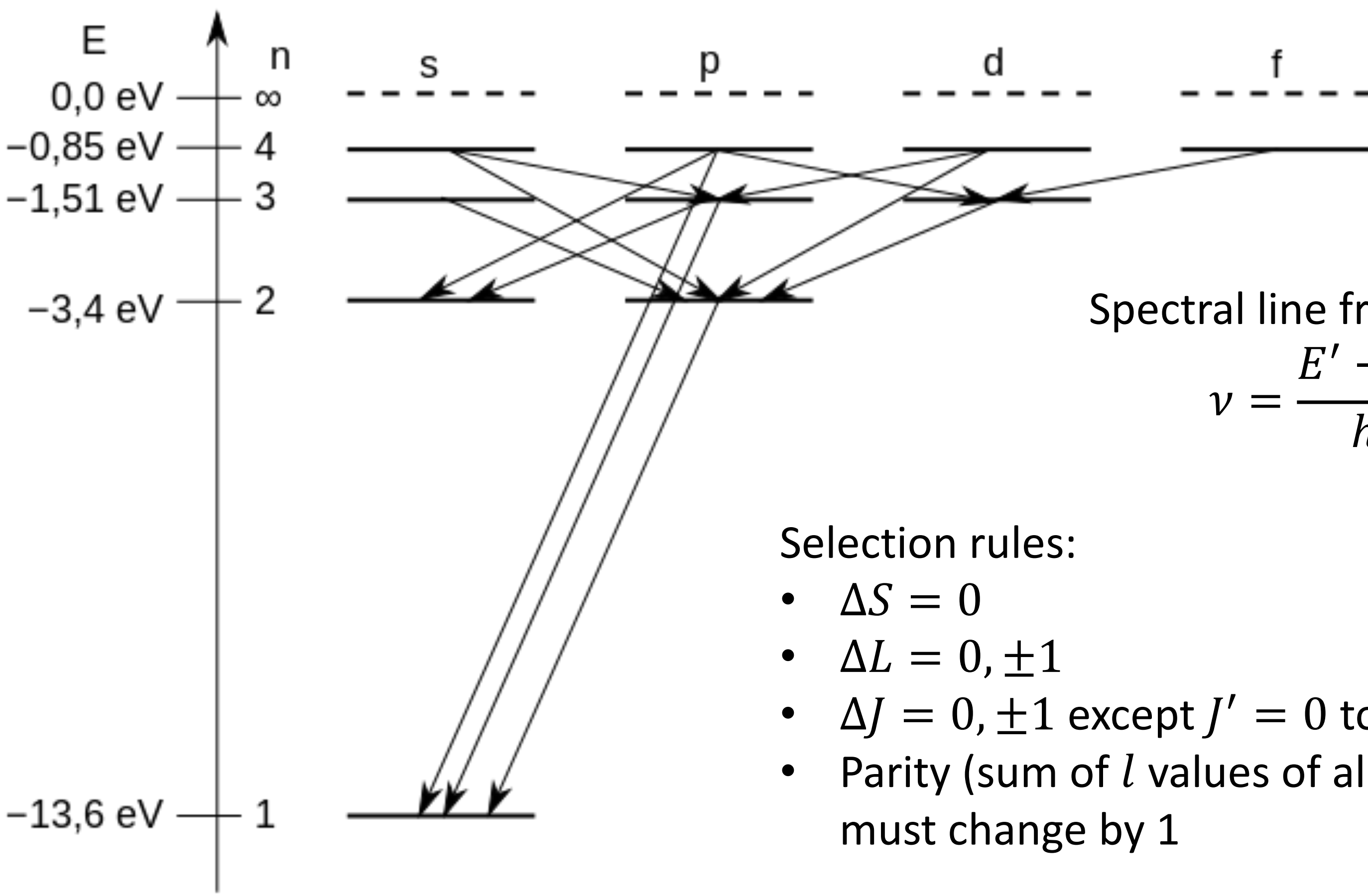

Spectral line frequency:

$$\nu = \frac{E' - E}{h}$$

Selection rules:

- $\Delta S = 0$
- $\Delta L = 0, \pm 1$
- $\Delta J = 0, \pm 1$ except $J' = 0$ to $J = 0$
- Parity (sum of l values of all electrons) must change by 1

More complicated system

An example from Lecture 11

e.g. **Fe XXI:** Fe ionized **20** times --- Z=26 nucleus w/ 6 electrons

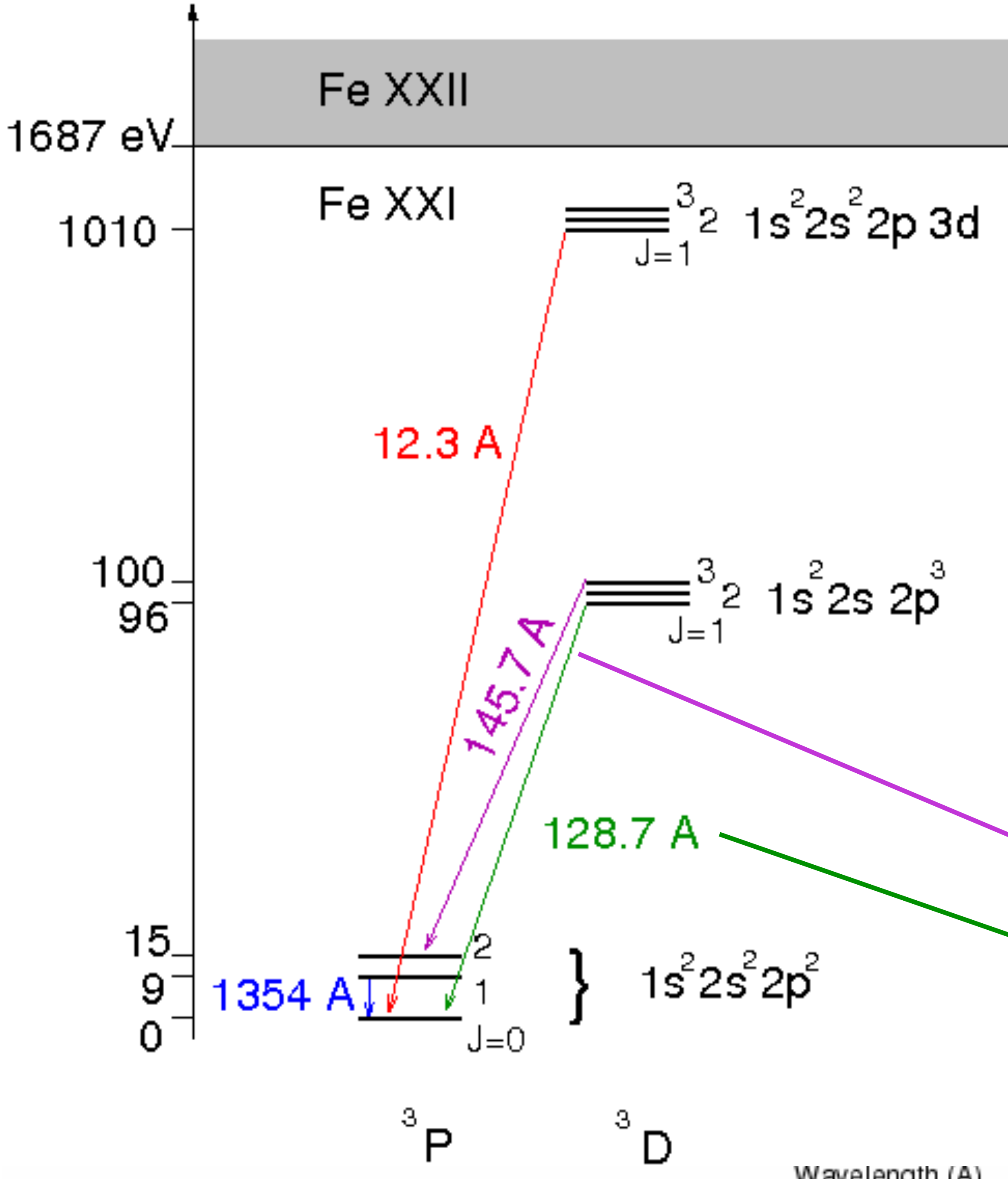

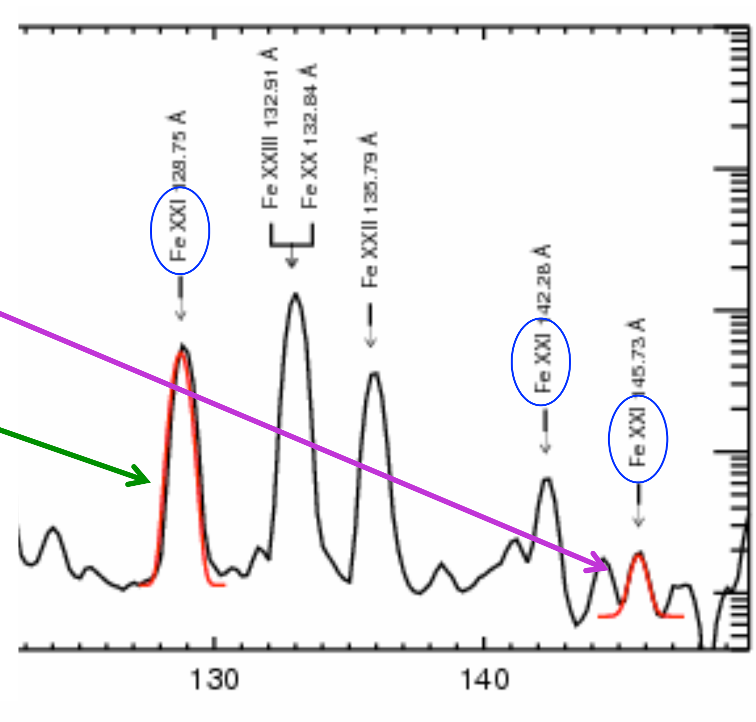

Basic atomic transition processes

- Discrete bound-bound transitions
    - $\lambda = hc/\Delta E$, where ΔE is the energy difference of the two levels
    - Result in discrete emission or absorption lines
- bound-free and free-bound (recombination) transitions
    - $\lambda = hc/\Delta E$, now $\Delta E = E_i + \frac{1}{2} m_e v_e^2$, where E_i is the ionization energy of the bound state
    - Produce series limit continua. E.g., Lyman and Balmer continua at $\lambda < 912$ Å and 3646 Å.
- Free-free (bremsstrahlung) radiation

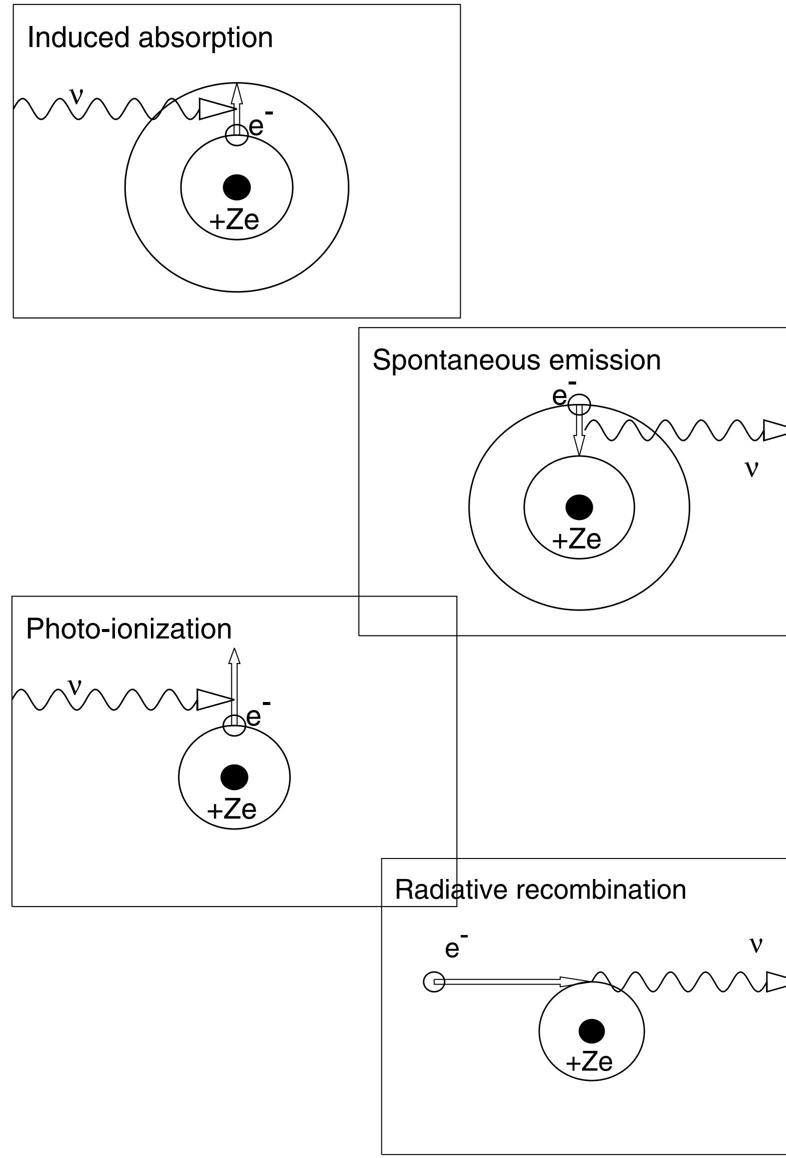

Line profiles

- Lorentzian:

$$I(\nu) \propto \frac{1}{(\nu - \nu_0)^2 + (\frac{\Delta\nu}{2})^2}$$

- Gaussian:

$$I(\nu) \propto \exp\left[-\left(\frac{2\sqrt{\ln 2}}{\Delta\nu}(\nu - \nu_0)\right)^2\right]$$

- $\Delta\nu$ determines the FWHM of the line
- Centroid position shift gives bulk velocity

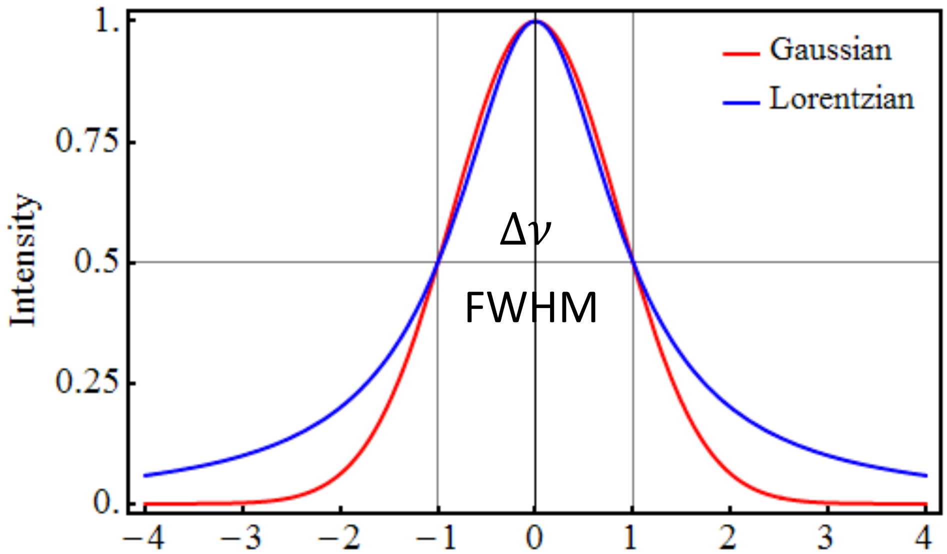

Line profile: natural broadening

- Heisenberg uncertainty principle:

$$\Delta E_u \Delta t_u \sim h/2\pi$$

$$\Delta E_u = h\Delta\nu_u$$

$$\Delta\nu_u = \frac{1}{2\pi}\frac{1}{\tau_u}$$

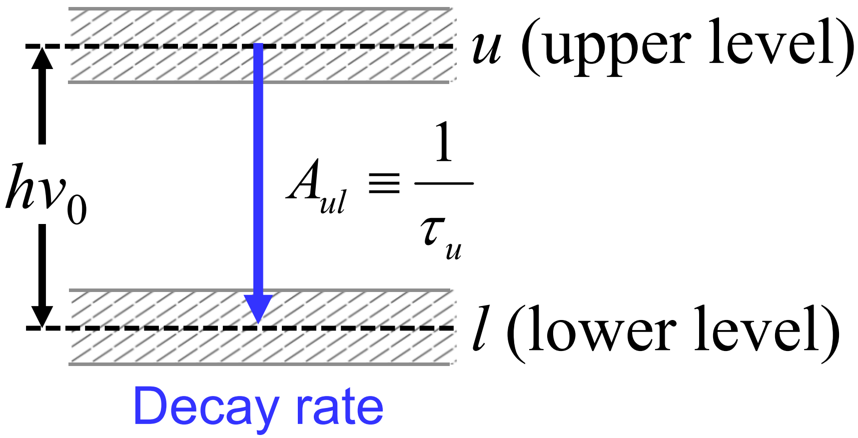

- In general

$$\Delta\nu_N = \Delta\nu_u + \Delta\nu_l = \frac{1}{2\pi}\left(\frac{1}{\tau_u} + \frac{1}{\tau_l}\right)$$

- Line shape function is ***Lorentzian***
- Line width is typically very small
  (e.g., 0.46 mA for H-alpha)

Line profile: collisional broadening

- Electron orbitals can be perturbed by collisions with other particles
- Characteristic time τ_c is the mean free time between collisions
- Line shape function – ***Lorentzian***:

$$I(\nu) = \frac{1}{\pi}\frac{\Delta\nu_c/2}{(\nu-\nu_0)^2+(\frac{\Delta\nu_c}{2})^2}$$

- Line width:

$$\Delta\nu_c = \frac{1}{2\pi}\left(\frac{1}{\tau_{c,u}}+\frac{1}{\tau_{c,l}}\right)$$

- Increases with density n and temperature T.

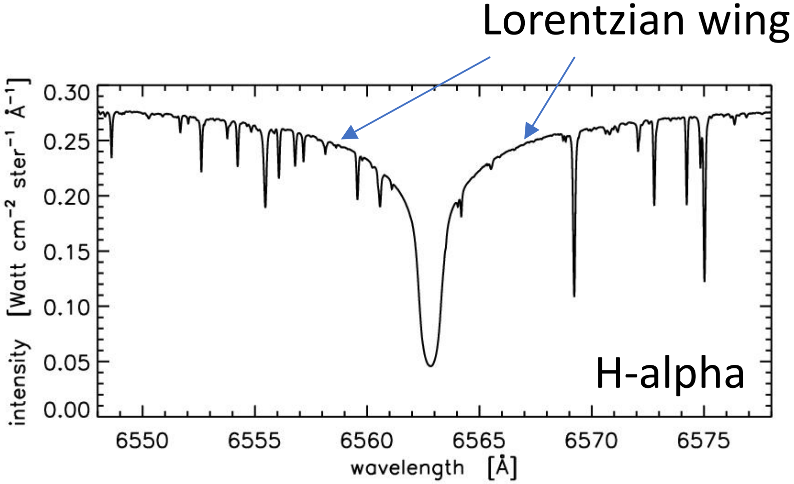

Line profile: Doppler broadening

- Moving particles see different frequency: Doppler shift
- Doppler shift: $\frac{\Delta\nu}{\nu} = \frac{v\cos\theta}{c}$
- Maxwellian velocity distribution for thermal plasma

$$df(v) = \left(\frac{m}{2\pi kT}\right)^{1/2} \exp\left(-\frac{mv^2}{2kT}\right) dv$$

- Line profile is ***Gaussian***:

$$I(\nu) \propto \exp\left[-\left(\frac{2\sqrt{\ln 2}}{\Delta\nu_D}(\nu - \nu_0)\right)^2\right],$$

where $\Delta\nu_D = 1.67\frac{\nu_0}{c}\sqrt{\frac{2kT}{m}}$ is the FWHM

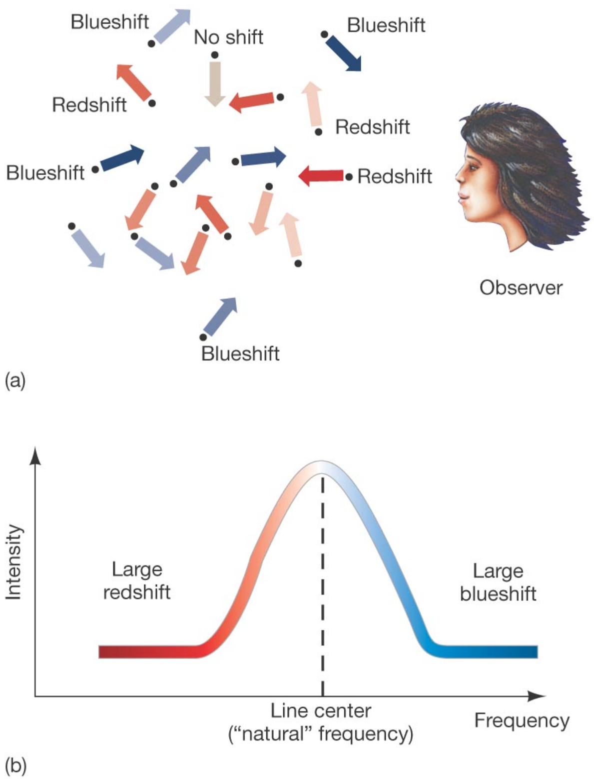

Line profile: Doppler broadening

- Additional Doppler broadening due to turbulent macroscopic bulk motions
- Assuming the turbulent velocity distribution is also Maxwellian with a rms velocity v_{rms}, the FWHM becomes:

$$\Delta\nu_D = 1.67\frac{\nu_0}{c}\sqrt{\frac{2kT}{m} + v_{rms}^2}$$

- The additional line width is sometimes referred to as ***non-thermal line width***

Line intensity: differential emission measure

Recap from lecture 11

- Line intensity:

$$I_\lambda = \int \frac{G_\lambda(T_e)}{d^2} DEM(T)dT$$

- $G_\lambda(T_e)$ is the contribution function of the given line (erg $cm^3\ s^{-1}\ sr^{-1}$), calculated from atomic physics (e.g., CHIANTI)
- I_λ is obtained from observation

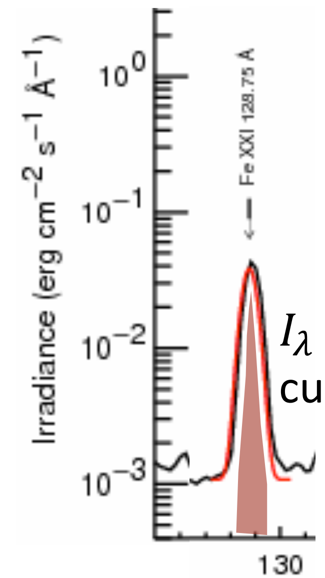

I_λ = Area under curve

From Lecture 11

DEM: EM loci approach

- Assume all the observed line intensity I_λ is produced by plasma with a total emission measure EM at a single temperature T_e

$$EM_{loci}(T_e) = I_\lambda / \frac{G_\lambda(T_e)}{d^2}$$

- $EM_{loci}(T_e)$ represents the upper limit of the true EM at this temperature. Such curves are known as ***EM loci*** curves
- Observation of multiple lines produces a set of EM loci curves, which constrain EM at different temperatures

Maximum EM (T)

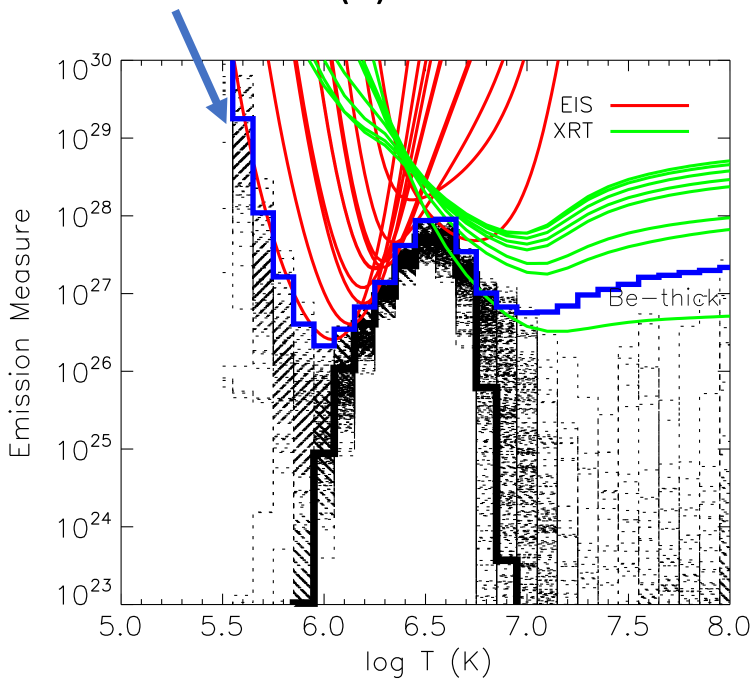

Winebarger et al 2011

DEM reconstruction

- Observations (recap from Lecture 11)
  - From spectral data: $I_\lambda = \int \frac{G_\lambda(T_e)}{d^2} DEM_V(T)dT$
  - From filter-graph images: $B = \int R(T)\, DEM_c(T)dT$
- N measurements ➡ N constraints on DEM(T)
- To form a DEM(T) curve, one needs many solutions at different T ➡ under-constrained problem
- Approaches
  - Reduce # of free parameters by prescribing the DEM curve to, e.g., one or multiple Gaussians (e.g., Aschwanden et al 2013) or interpolated spline function (e.g., the Hinode/XRT method)
  - Monte-Carlo forward-fitting (e.g., Kashyap & Drake 1998)
  - Regularized inversion (Hannah & Kontar 2012)

line ratio diagnostics

- Certain line intensity ratios for a given ion can be used for density or temperature diagnostics
- At low densities, collisional de-excitation ($C_{ul}n_u$) is not important, collisional excitation ($C_{lu}n_l$) is balanced by spontaneous emission ($A_{ul}n_u$)

$$\frac{\varepsilon_{31}}{\varepsilon_{21}} = \frac{E_{31}A_{31}N_3}{E_{21}A_{21}N_2} = \frac{E_{31}C_{13}N_1}{E_{21}C_{12}N_1} \sim \frac{C_{13}}{C_{12}} \sim \frac{\Omega_{13}}{\Omega_{12}} \exp\left(\frac{-E_{23}}{kT}\right)$$

(let's ignore transitions between levels 2 & 3)

Temperature dependence

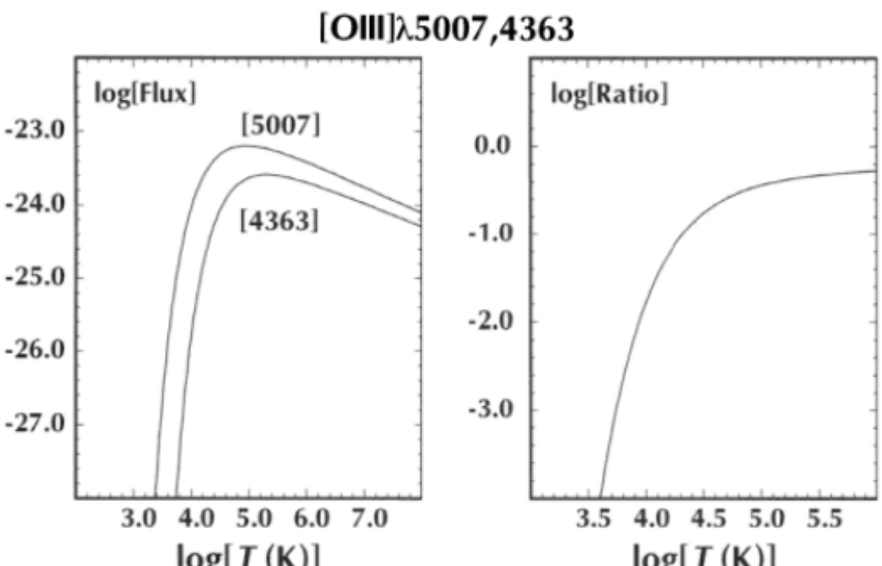

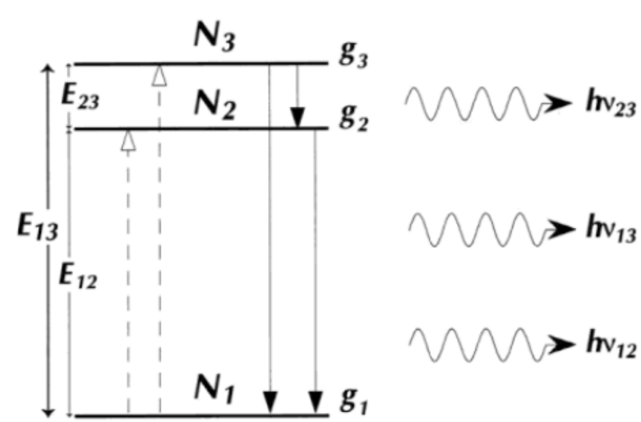

Line ratio diagnostics

- At high densities, collisional de-excitation becomes important.
- The radiative depopulation rate becomes negligible comparing to the collisional de-excitation. At the limit of LTE:

$$\frac{N_u}{N_l} = \frac{g_u}{g_l} \exp\left(\frac{-E_{ul}}{kT}\right)$$

- Now the line ratio achieves another limit

$$\frac{\varepsilon_{31}}{\varepsilon_{21}} = \frac{E_{31}A_{31}N_3}{E_{21}A_{21}N_2} = \frac{E_{31}A_{31}g_3}{E_{21}A_{21}g_2} \exp\left(\frac{-E_{23}}{kT}\right)$$

Observation from Hinode/EIS

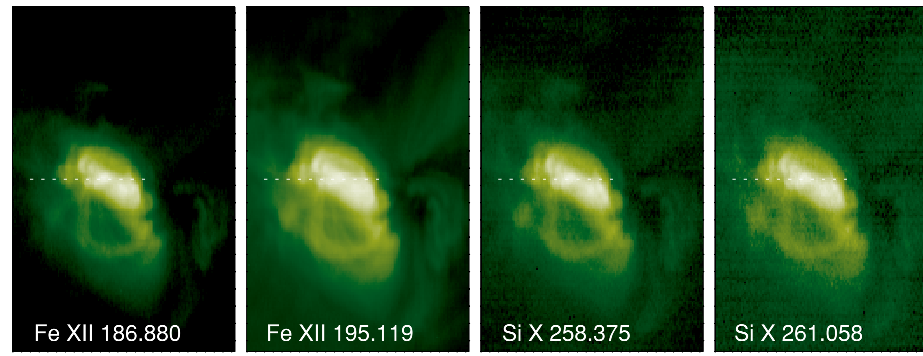

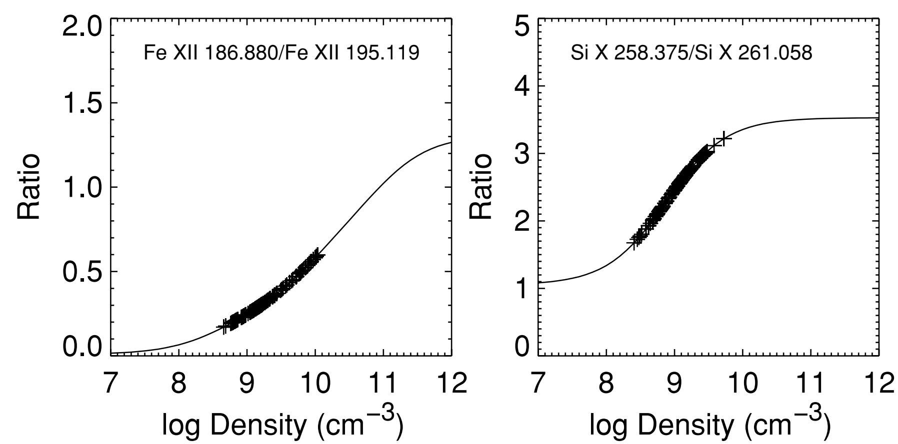

Warren et al 2010

Flare spectroscopy: Instrumentation*

- Instrumentation:
  - (Extreme) Ultraviolet: SOHO/CDS, SOHO/SUMER, Hinode/EIS, IRIS, SDO/EVE…
  - Radio, optical, X-ray: VLA, EOVSA, BBSO, DST, RHESSI, Fermi…
- Current capabilities allow spatially-resolved line profiles to be obtained
  - Along a movable slit (diffraction grating): Hinode/EIS, IRIS, BBSO…
  - Fabry-Perot narrow-band imager: BBSO, DST…
  - Fourier transform: radio imaging spectrometers (VLA, EOVSA...)

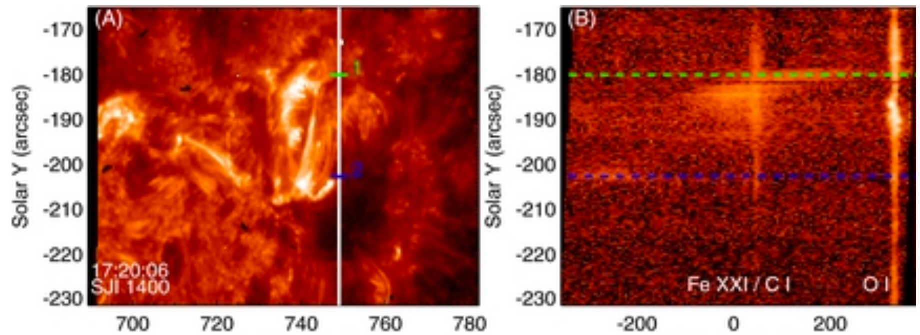

IRIS (Tian et al 2014)

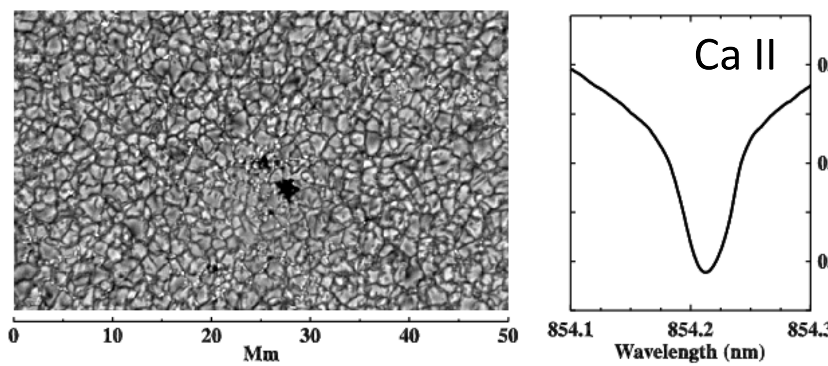

DST/IBIS

*not an exhaustive list

EIS observation of explosive evaporation

EIS offers 10s of lines covering 10^4-10^7 K

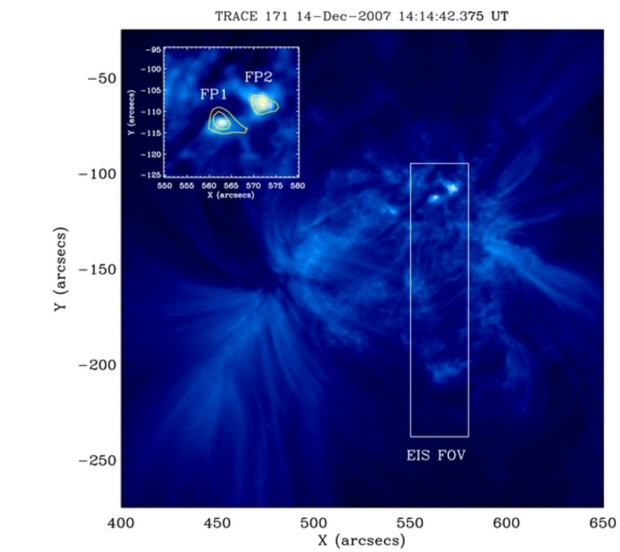

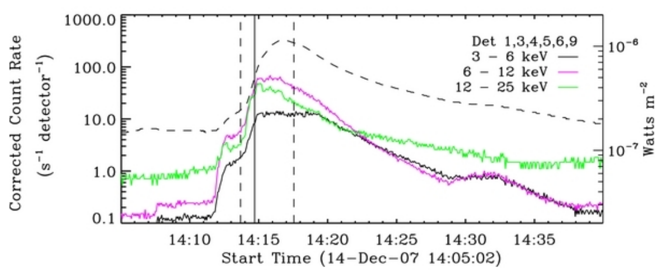

Fe XV (~2 MK) Intensity

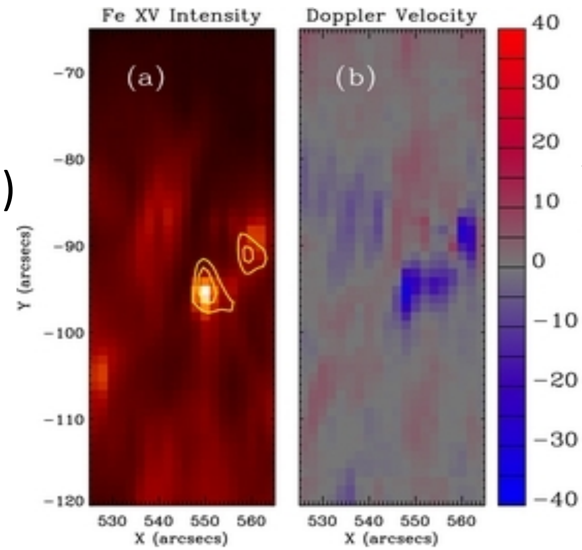

Doppler velocity

Nonthermal line width

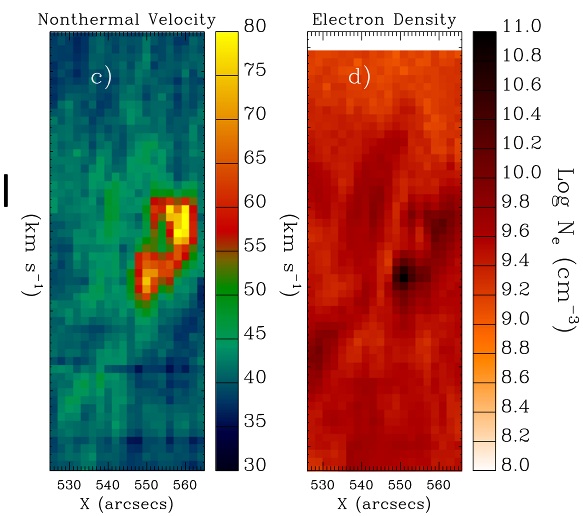

Density from Fe XIV line ratio

During the flare impulsive phase, plasma at the HXR footpoints was hot, upflowing, turbulent, and dense ➡ Chromospheric evaporation

Milligan 2011

Evaporation speed vs. temperature

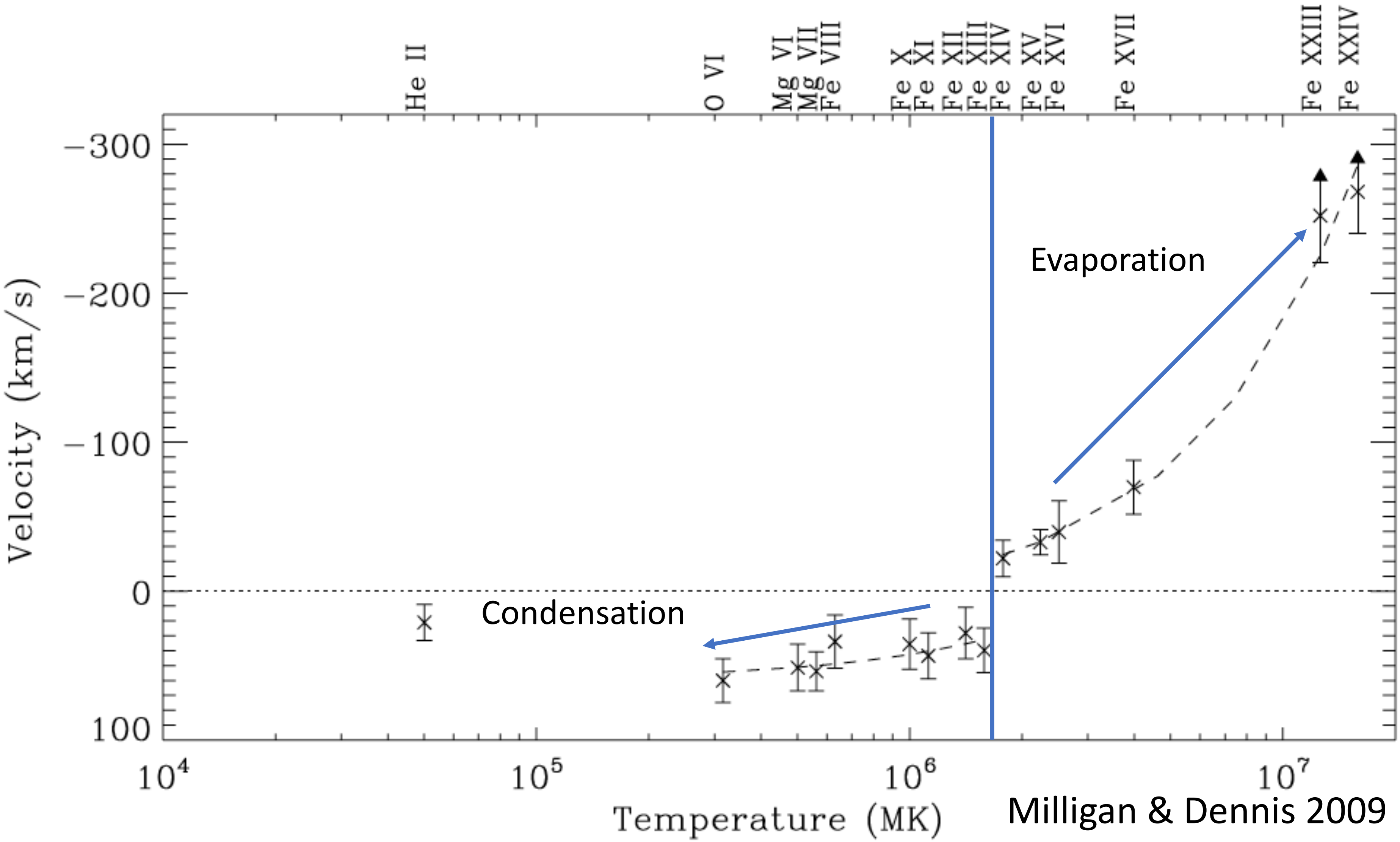

Milligan & Dennis 2009

From HXR observations: $F_{fl} \geq 5 \times 10^{10}$ erg cm^{-2} s^{-1} $> F_{cr}$ → Explosive Evaporation

Comparing to explosive evaporation model

- Upflow speed increases with T
- Downflow speed shows a weaker dependence on T
- Both are predicted by the models
- The “Flow Reverse Point” is where most of the electron energy is dumped into the chromosphere

The corresponding T (~1.5 MK) is a bit too high comparing to the Fisher model

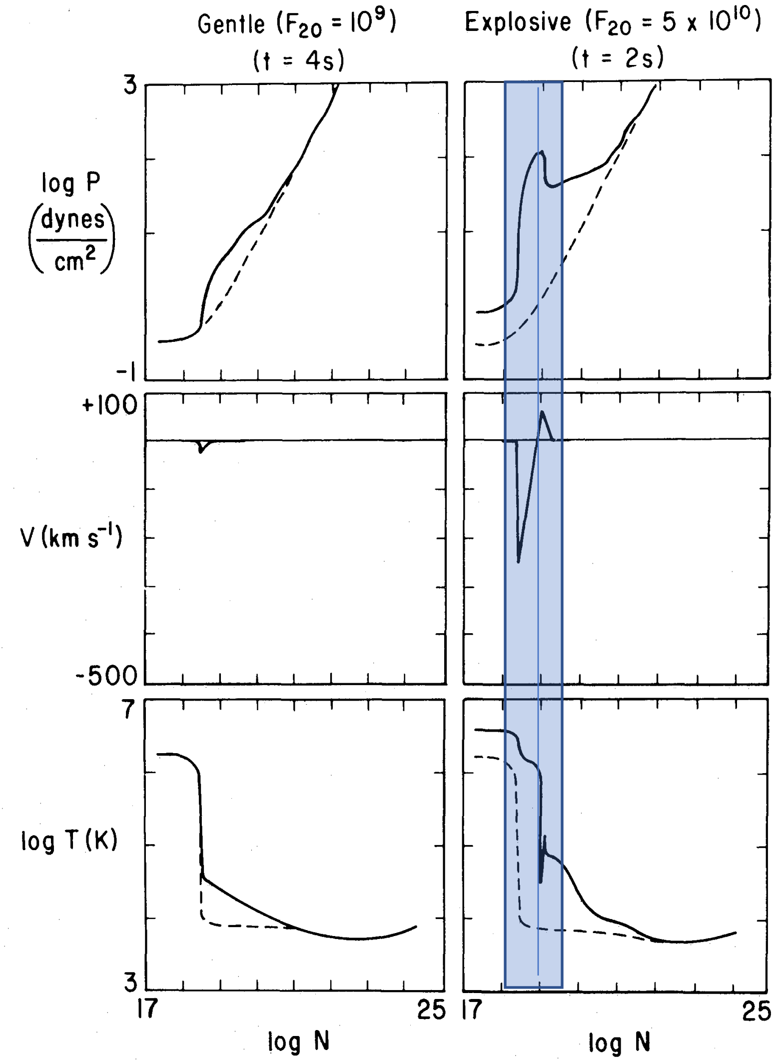

Fisher et al 1985 (see also Lecture 11)

Comparing to explosive evaporation model

- Upflow speed increases with T
- Downflow speed shows a weaker dependence on T
- Both are predicted by the models
- The "Flow Reverse Point" is where most of the electron energy is dumped into the chromosphere

The corresponding T (~1.5 MK) is a bit too high comparing to the Fisher model

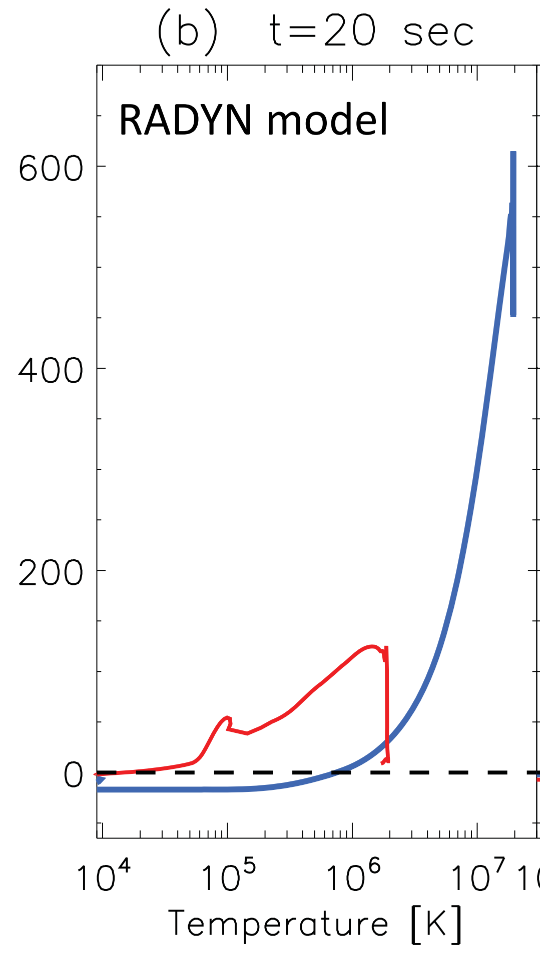

Rubio da Costa et al 2015

Observation of gentle evaporation

- For $F_{fl} < F_{cr}$, "gentle evaporation", no associated downflows

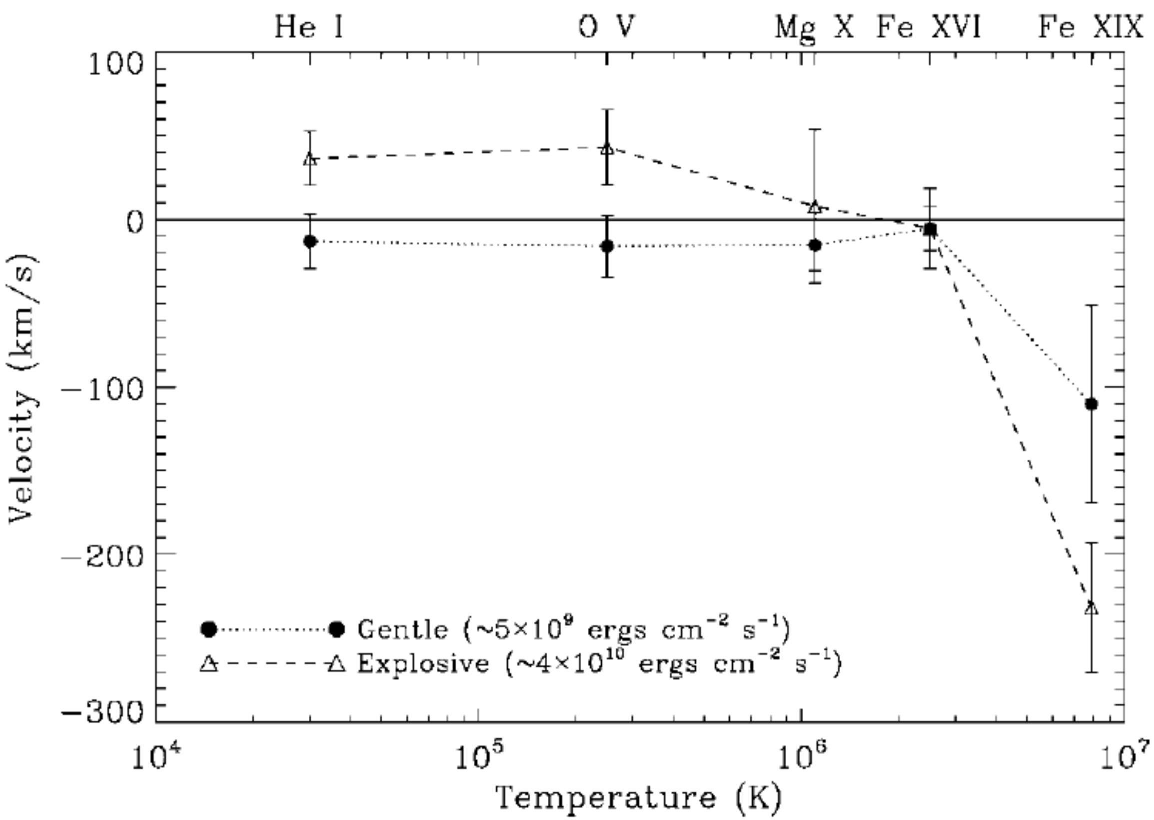

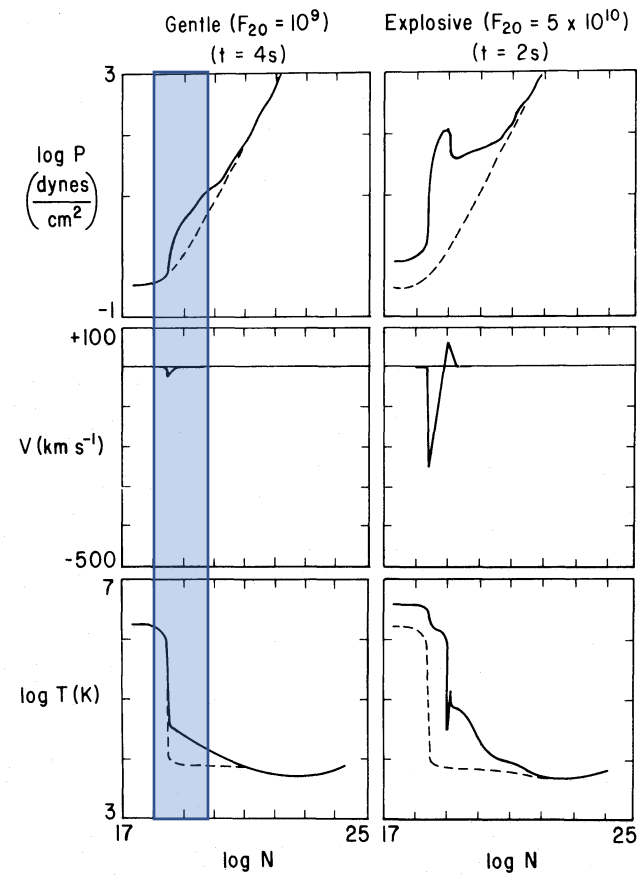

Milligan et al 2006

Chromospheric Evaporation: IRIS observations

- IRIS provides high spatial resolution, time cadence, and sensitivity
- Provides one hot line (Fe XXI; ~10 MK) sensitive to flaring plasma and many cool lines for chromospheric/transition region plasma

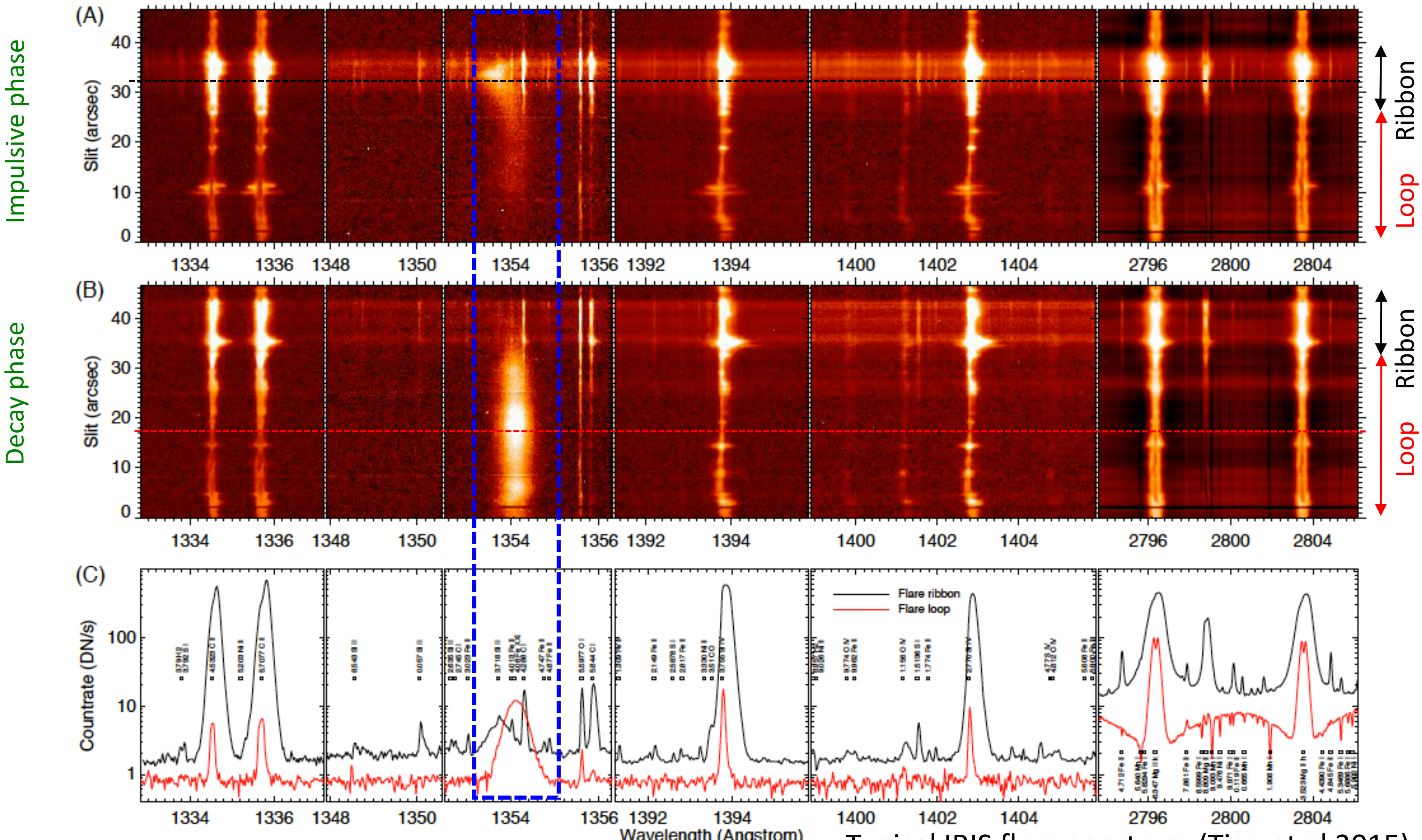

Typical IRIS flare spectrum (Tian et al 2015)

UV continuum emission from flare ribbon

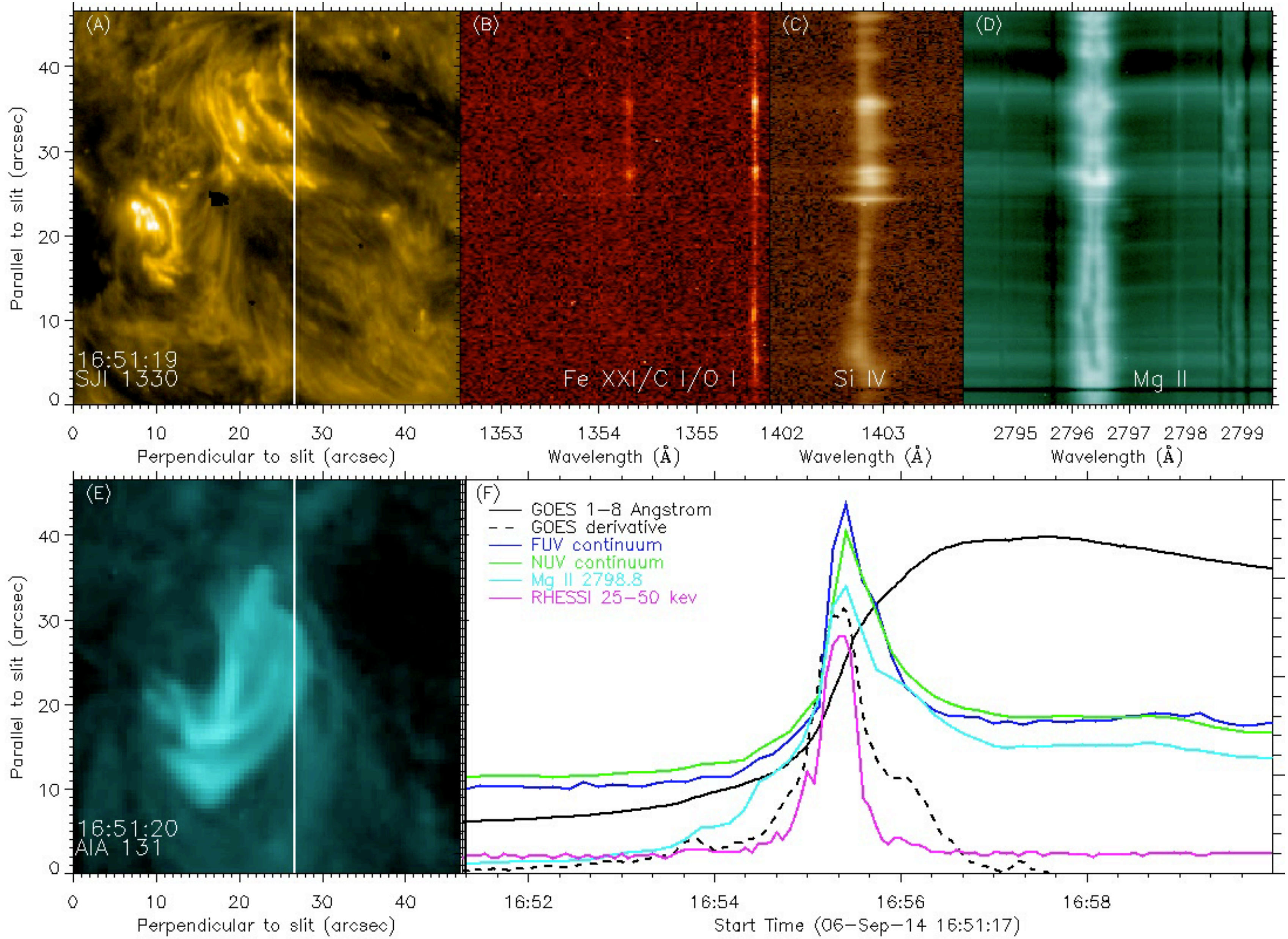

Tian et al. ApJ, 2015

Evaporation speed and energy release rate

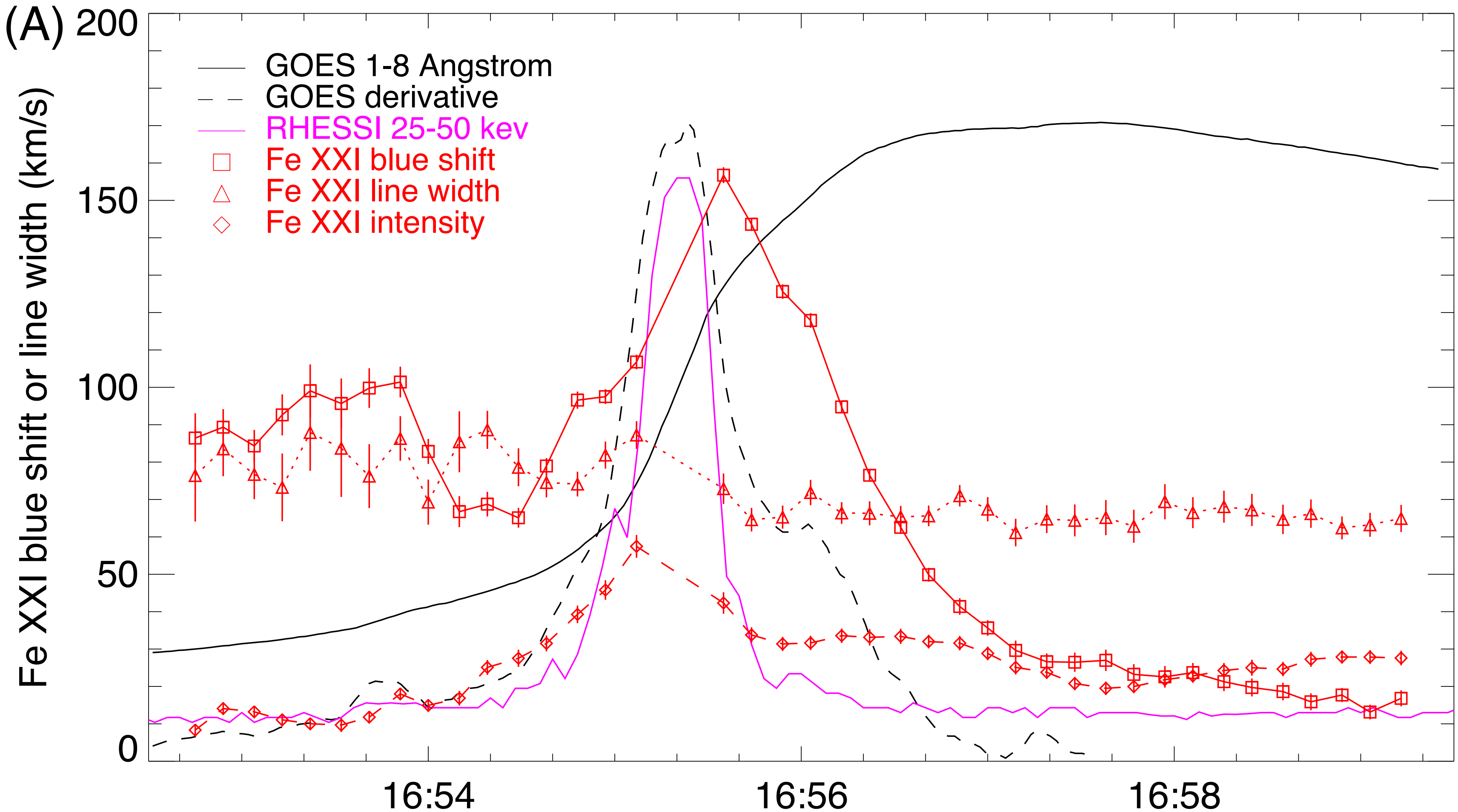

Fe XXI blue shift is correlated with HXR or SXR derivative

(Tian et al. ApJ, 2015; Li et al. ApJ, 2015)

Chromospheric evaporation: temporal evolution

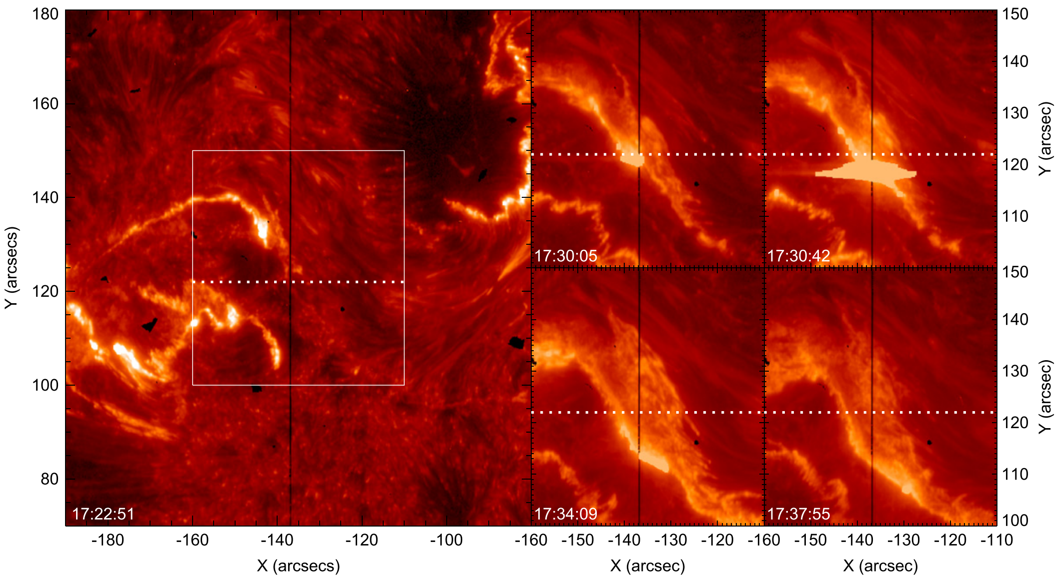

Fe XXI

Mg II

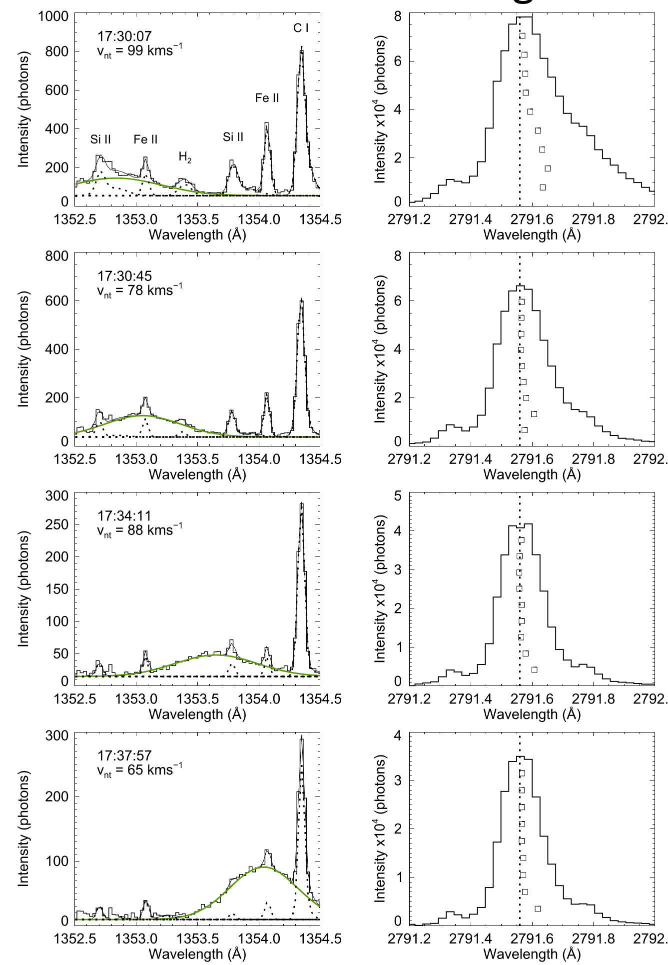

Graham & Cauzzi 2015

Chromospheric evaporation: temporal evolution

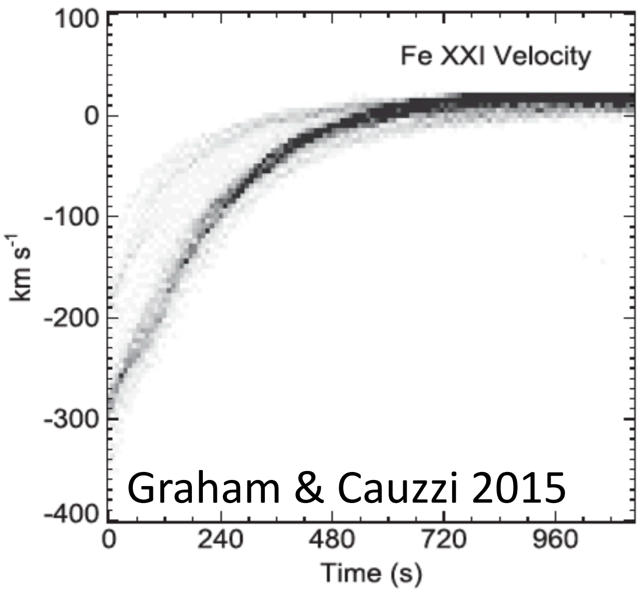

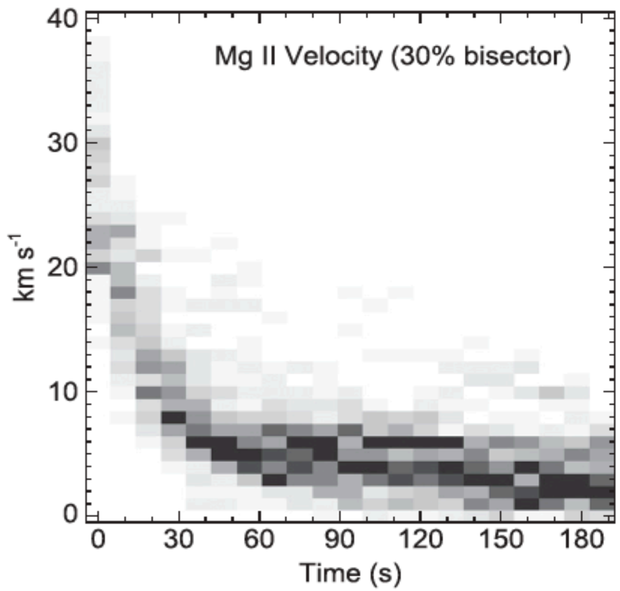

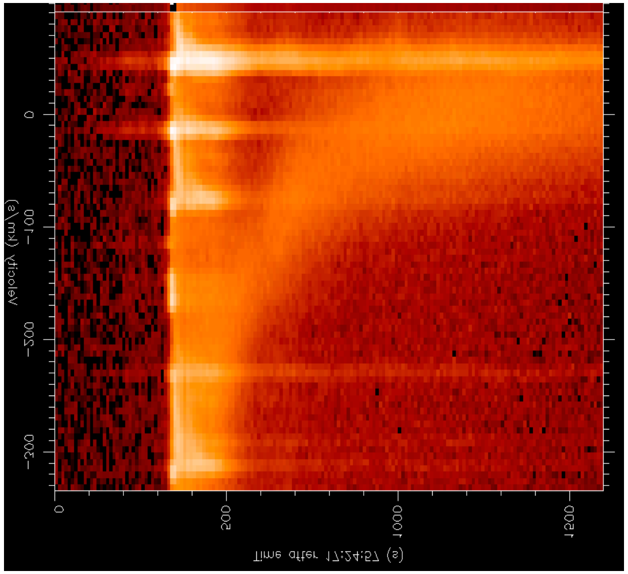

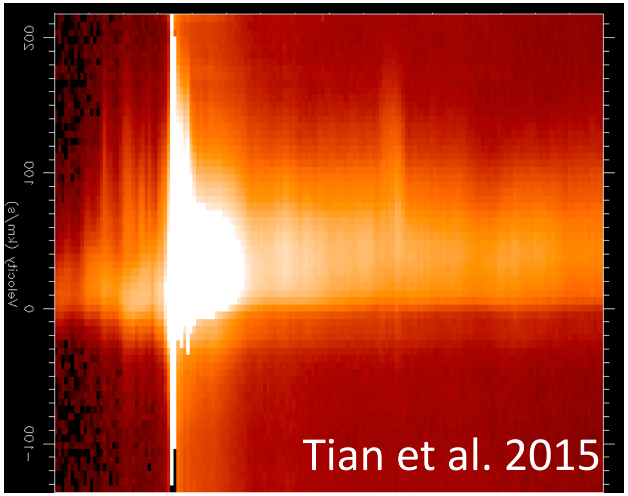

- Fe XXI blue shift slows down after impulsive phase
- Si IV redshift also slows down, but more rapidly
- Consistent with modeling results
- But maximum evaporation lags behind condensation by ~68 s

Flows around the reconnection site

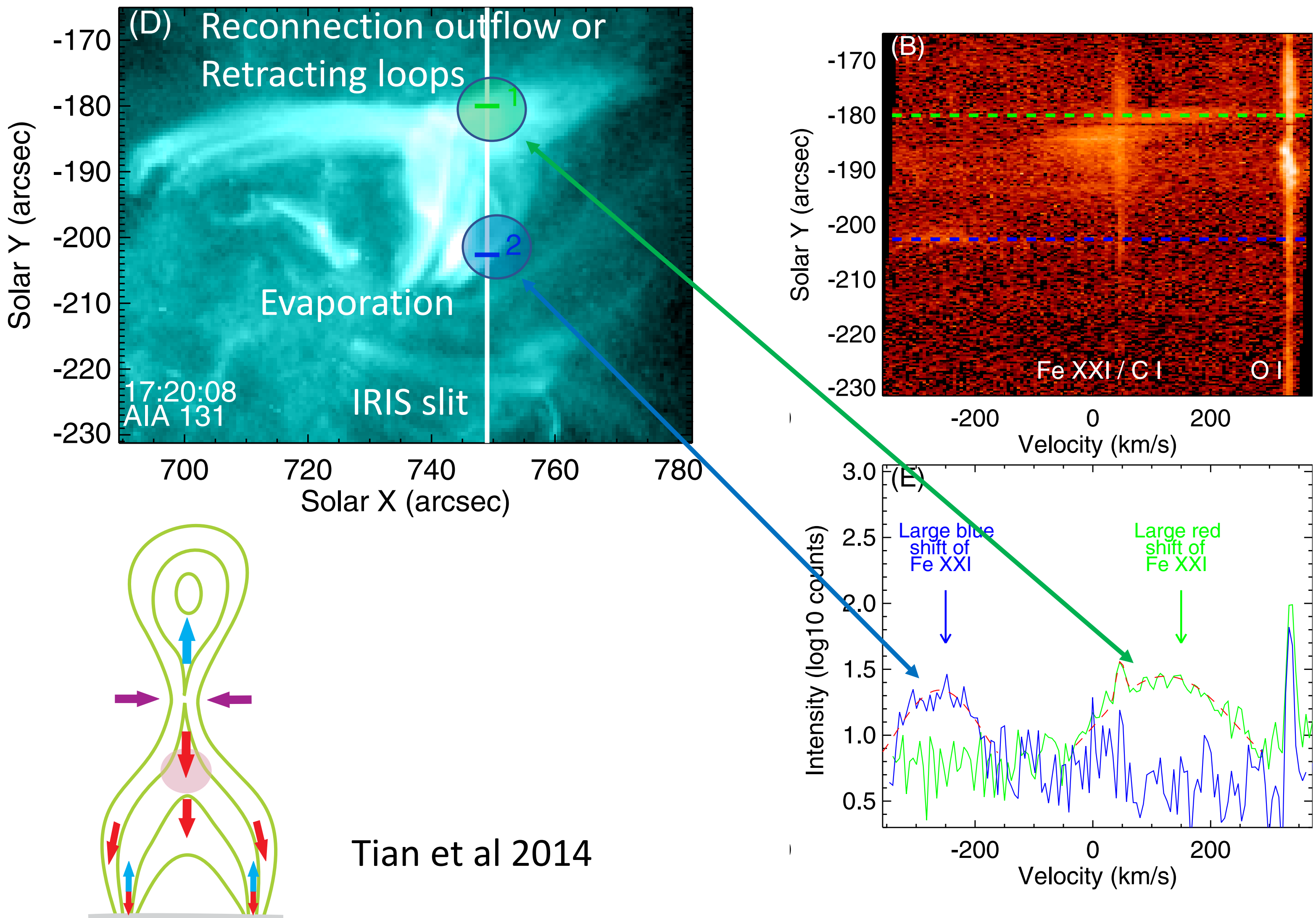

Tian et al 2014

Summary

- Atomic structure basics
- Emission lines provide rich diagnostics
  - Line profile diagnoses bulk flow and Doppler width
  - Line intensity diagnoses density, temperature, DEM
- Spatially-resolved (E)UV spectroscopy is a great tool for studying thermal flare plasma
- Following weeks: nonthermal particles and radiation, where radio/X-ray spectroscopy plays an important role